

Characteristics of Boron Diffusion in Polysilicon/Silicon Systems with a Thin Si-B Layer as Diffusion Source

T. P. Chen, T. F. Lei, H. C. Lin, and C. Y. Chang

Department of Electronics Engineering and Institute of Electronics, National Chiao Tung University, and National Nano Device Laboratory, Hsinchu, Taiwan

ABSTRACT

A new material, Si-B layer, as boron diffusion source for polysilicon/silicon systems, has been investigated. The Si-B layer was deposited on polysilicon in an ultrahigh vacuum chemical vapor deposition (UHV/CVD) system at 550°C. The characteristics of boron diffusion in Si-B layer/polysilicon/silicon systems have been investigated by using secondary ion mass spectroscopy (SIMS) and cross-sectional transmission electron microscopy (XTEM). To remove the Si-B layer after the drive-in step, the Si-B layer was oxidized completely during thermal drive-in stage and removed with a diluted hydrofluoric acid. The effects of thermal oxidation of Si-B layer on boron diffusion profiles and polysilicon structures were analyzed. It was found that the boron profiles within the polysilicon are slightly dependent on the oxidation of Si-B layer. Moreover, the polysilicon grain size for Si-B layer source were enlarged, as compared with conventional BF_3^+ -implanted polysilicon source. It is attributed to the effects of the gettering of oxygen impurity by the Si-B layer and secondary grain growth during Si-B layer oxidation. In addition, the boron diffusion profiles in the silicon substrate for Si-B layer source exhibited a more shallow junction depth and less sensitivity to the thermal budget, as compared with BF_3^+ -implanted polysilicon source. This is considered to be the effect of the smaller surface concentration, C_s , in the silicon substrate for Si-B layer source.

Introduction

Complementary bipolar CMOS (C-BiCMOS) circuit have advantages for both digital and analog application; hence, it is important to study the characteristics of p-n-p polysilicon emitter bipolar transistors.¹⁻³ Conventionally, the heavily p⁺ polysilicon films are often doped by the BF_3^+ implantation and driven into silicon substrate in high temperature processes.^{3,4} It is well known that the morphology of polysilicon/silicon interface plays an important role in shaping the diffusion profiles of doping impurity and the electrical properties polysilicon emitter bipolar transistors.¹⁻⁶ Recently, it was found that the incorporation of fluorine atoms in the polysilicon films during BF_3^+ implantation has the effect of accelerating the breakup of polysilicon/silicon interfacial oxide.⁷ However, the breakup of interfacial oxide loses the improvement of dc current gain of bipolar transistors.⁸ Moreover, in our recent studies, it was observed that two groups of fluorine bubbles are distributed in the as-implanted fluorine peak region and at the original polysilicon/silicon interface.⁹ The presence of fluorine bubbles at the polysilicon/silicon interface affects the transport of majority and minority carrier in the emitter region. For boron-implanted polysilicon/silicon systems, it was found the boron profiles and the junction depth are sensitive to the dopant dose.^{10,11} Moreover, the high dopant dose may require undesirably long implantation times. Therefore, a new technique to form more shallow and uniform junctions is necessary.

In our previous studies, we have shown that an Si-B layer can be deposited in a UHV/CVD system at low temperature (550°C).¹² Auger electron spectroscopy (AES) and secondary ion mass spectroscopy showed that boron concentration is extraordinarily high. From the analysis of transmission-electron diffraction, the phase of silicon hexaboride (SiB_6) was found to be present in the as-deposited Si-B layer. The results indicated that Si-B layer can be regarded as an infinite diffusion source of boron atoms. Recently, it was found that the Si-B layer source diodes exhibit a shallower junction depth and better I-V characteristics than conventional BF_3^+ -implanted polysilicon source diodes.¹³ Here, we investigate the characteristics of boron diffusion profiles in the polysilicon/silicon system by using a thin Si-B layer as diffusion source.

Experimental

The substrates used in this experiment were n-type, (100) Si wafers with a resistivity of 0.5 to 2 $\Omega\text{-cm}$. Prior to polysilicon deposition, all wafers were dipped in a dilute HF solution to remove surface native oxide followed by a

deionized water rinse. Then, polysilicon films with a thickness of 3500 Å were deposited in a low pressure chemical vapor deposition (LPCVD) system at 625°C using SiH_4 gas. The deposition pressure and deposition rate were 180 ~ 220 mTorr and 110 Å min^{-1} , respectively. During the LPCVD polysilicon deposition process, a native oxide was formed at the polysilicon/silicon interface. After polysilicon deposition, all wafers were cleaned and loaded into the loading chamber of UHV/CVD system after a diluted HF dip, and then transferred into the reaction chamber. The UHV/CVD system is an isothermal hot-wall system that consists of a reaction chamber and a loading chamber. The base pressure of the reaction chamber is 2×10^{-8} Torr. The Si-B layer with a thickness of 350 Å was grown by using a mixture of pure SiH_4 and B_2H_6 (1% in H_2) at 550°C. The gas ratio of $\text{B}_2\text{H}_6/\text{SiH}_4$ and gas pressure were 1 and 1.51 mTorr, respectively. After Si-B layer deposition, all wafers were annealed in the temperature range of 900 to 1000°C. During the drive-in stage, some boron atoms diffused from Si-B layer into polysilicon and single-crystal silicon to form p⁺-n junction and the Si-B layer was oxidized completely. For comparison, BF_3^+ implanted-polysilicon/silicon (80 keV, $6 \times 10^{15} \text{ cm}^{-2}$) was annealed in the temperature range of 900 to 1000°C. Finally, the thickness of Si-B layer and structure morphology of Si-B layer/polysilicon/silicon substrate were examined by cross-sectional transmission electron microscopy (XTEM) using a

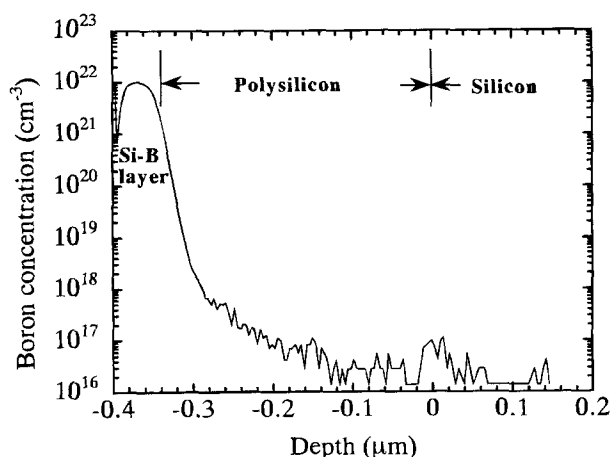


Fig. 1. SIMS boron depth profiles of as-deposited Si-B layer on polysilicon/silicon.

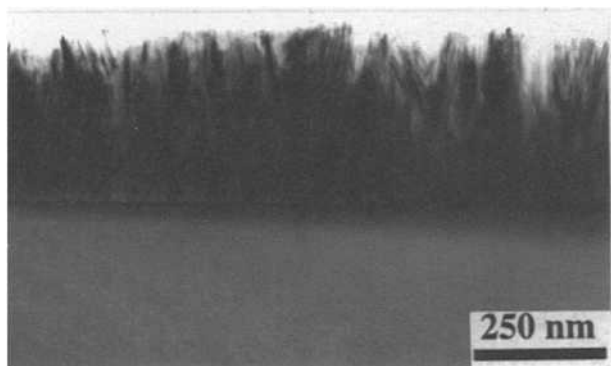


Fig. 2. Cross-sectional TEM micrograph of an Si-B layer/polysilicon/silicon substrate structure.

JEOL 200 CX microscope, operating at 200 keV. The analysis of boron distribution profiles were carried out with a CAMECA IMS-4f ion microanalyzer using O_2^+ primary ion bombardment.

Results and Discussion

Characteristics of as-deposited Si-B layer on polysilicon.—Figure 1 shows the SIMS boron depth profiles of as-deposited Si-B layer on polysilicon/silicon. The boron concentration of Si-B layer is extraordinarily high and an abrupt transition boron profile between Si-B layer and polysilicon can be obtained by UHV/CVD techniques. Figure 2 shows the cross-sectional TEM micrograph of an Si-B layer/polysilicon/silicon substrate structure. The interface of Si-B layer/polysilicon is free of oxide. It is deduced that the diffusion of boron between Si-B layer and polysilicon is free of an interfacial oxide barrier. The absence of interfacial oxide is attributed to the passivation of surface dangling bonds of polysilicon silicon by hydrogen atoms to form hydrogen-silicon bonds after an HF solution etching.¹⁴ This hydrogen passivation layer effectively retards the oxidation of polysilicon surface before the deposition of UHV/CVD layers. Moreover, the analysis of transition electron diffraction pattern showed that the phase of silicon-hexaboride (SiB_6) was found to be presented in as-deposited Si-B layer.¹²

Diffusion behavior of B in the Si-B layer/polysilicon/silicon.—Figure 3 shows the SIMS boron depth profiles in the Si-B layer/polysilicon/silicon structures after thermal annealing in an N_2 ambient at 900°C for 30 min. As mentioned previously, the diffusion of boron from the Si-B layer into polysilicon is free of interfacial oxide barrier. Some boron atoms diffused from the Si-B layer into polysilicon during the thermal drive-in stage. At the same time, the boron

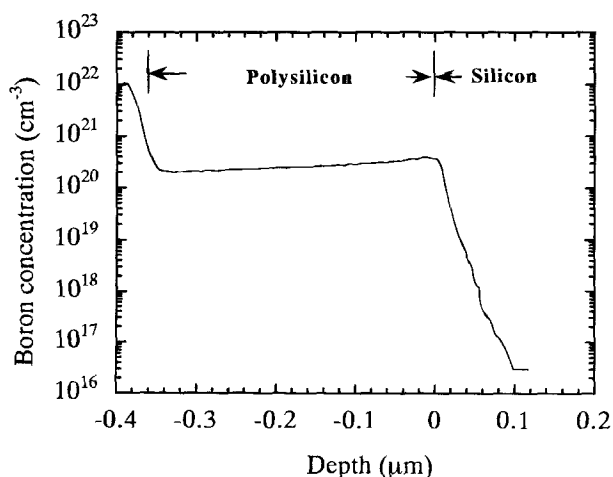


Fig. 3. SIMS boron depth profiles of Si-B layer/polysilicon/silicon after thermal annealing in an N_2 ambient at 900°C for 30 min.

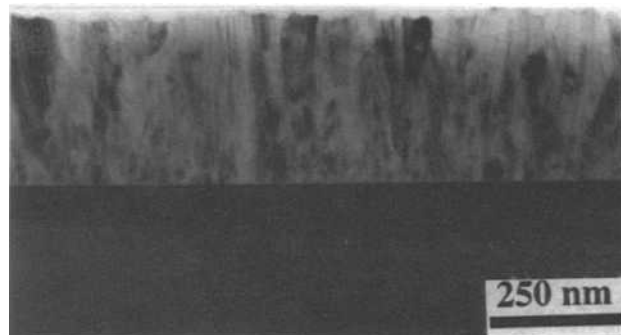


Fig. 4. Cross-sectional TEM micrograph of an Si-B layer/polysilicon/silicon substrate structure after thermal annealing in an N_2 ambient at 900°C for 30 min.

atoms transport across the polysilicon/silicon interface into silicon substrate to form a shallow junction in the silicon substrate. Moreover, the Si-B layer remained on the polysilicon surface after the thermal drive-in stage. It has been reported that the boron diffusivity is strongly reduced in single-crystal silicon and polysilicon where the boron concentration exceeds the solid solubility limit.^{3,15,16} In our previous studies, we have shown that the presence of SiB_6 in the Si-B layer may lead to the reduction of boron diffusivity in the Si-B layer during thermal annealing.¹² Therefore, most boron atoms are immobile in the thin Si-B layer during thermal annealing. This implies that boron released from the Si-B layer diffuses in polysilicon and is finally mainly located in grain boundaries. The boron profile within the polysilicon film exhibits a gradual increase of boron concentration toward the polysilicon/silicon interface. The phenomenon also was observed for boron-implanted polysilicon and *in situ* doped polysilicon as diffusion sources.^{10,11,17} The XTEM micrograph, Fig. 4, reveals a smaller polysilicon grain size near the polysilicon/silicon interface. Therefore, it is explained by the effect of nonuniform grain size distribution and the segregation of boron atoms in the polysilicon grain boundary.^{10,18} Rausch *et al.*¹⁹ showed the segregation of boron into the polysilicon with a segregation coefficient of 0.7.

Oxidation of Si-B layer.—As mentioned previously, the Si-B layer remained on the polysilicon surface after the thermal drive-in process. However, it was found that the high boron concentration layer exhibits a high resistivity.²⁰ The Si-B layer increases the series resistance for device applications. Therefore, it is desired to remove the Si-B layer after the thermal drive-in process. A process to remove Si-B layer during drive-in stage was developed in this study. It was found that the Si-B layer was easily oxidized in wet oxygen atmosphere. Figure 5a shows the SIMS boron profile as a function of sputtering time for Si-B layer/polysilicon/silicon system after thermal annealing at 900°C for 35 min in an N_2 ambient and 5 min in a wet O_2 ambient. Si-B layer was oxidized and the oxide layer contains high boron concentration. From the analysis of Fourier transform infrared spectroscopy (FTIR), the Si-B oxide layer reveals the absorption band of the Si-O at 9.2 and B-O at 7 μm . Therefore, the Si-B oxide layer is considered to be the mixing of SiO_2 and B_2O_3 .²¹ The Si-B oxide layer was easily removed with a diluted HF solution. Figure 5b shows the boron depth profile of Fig. 5a after removing the Si-B oxide layer. The SIMS boron depth profile demonstrated that the Si-B layer was completely removed by this technique. Moreover, whether the Si-B layer is present can be determined by the nature of surface. The surface of Si-B layer was found to be hydrophilic even after a diluted HF solution dip;^{12,21} however, the surface of polysilicon exhibits a hydrophobic nature.

Influence of thermal oxidation of Si-B layer on boron diffusion profiles.—The effects of thermal oxidation of Si-B layer on the boron diffusion profile in the polysilicon/silicon system have been investigated as a function of differ-

ent thermal processes. Three groups of wafers were annealed at 900°C for 30 min. The detailed drive-in process of sample A, B, and C is as follows: sample A: 5 min in an N₂ ambient, 5 min in a wet O₂ ambient, and 20 min in an N₂ ambient; sample B: 15 min in an N₂ ambient, 5 min in a wet O₂ ambient, and 10 min in an N₂ ambient; and sample C: 25 min in an N₂ ambient and 5 min in a wet O₂ ambient.

Figure 6 shows the boron depth profiles of samples A, B, and C in the polysilicon/silicon after removing the Si-B oxide layer. Comparing the three curves in Fig. 6, the shape of boron profiles and the junction depth in the silicon substrate are almost the same for samples A, B, and C. The boron profiles of sample A, B, and C, compared with Fig. 3, indicate that the diffusion of boron was slightly enhanced by the wet oxidation of Si-B layer. The boron profiles within the polysilicon films exhibited a gradual increase of boron concentration toward the polysilicon/silicon interface and a discontinuity of boron profiles at the polysilicon/silicon interface for all samples. Moreover, the tendency of increasing boron concentration and the discontinuity of boron profile are most pronounced for sample C and least pronounced for sample A. As mentioned previously, the increasing boron concentration is attributed to the nonuniform grain size distribution in the polysilicon film and the segregation of boron atoms in the polysilicon grain boundary. Moreover, Rausch *et al.*¹⁹ have shown that the discontinuity of boron profiles at the polysilicon/silicon interface is caused by the segregation of boron in the

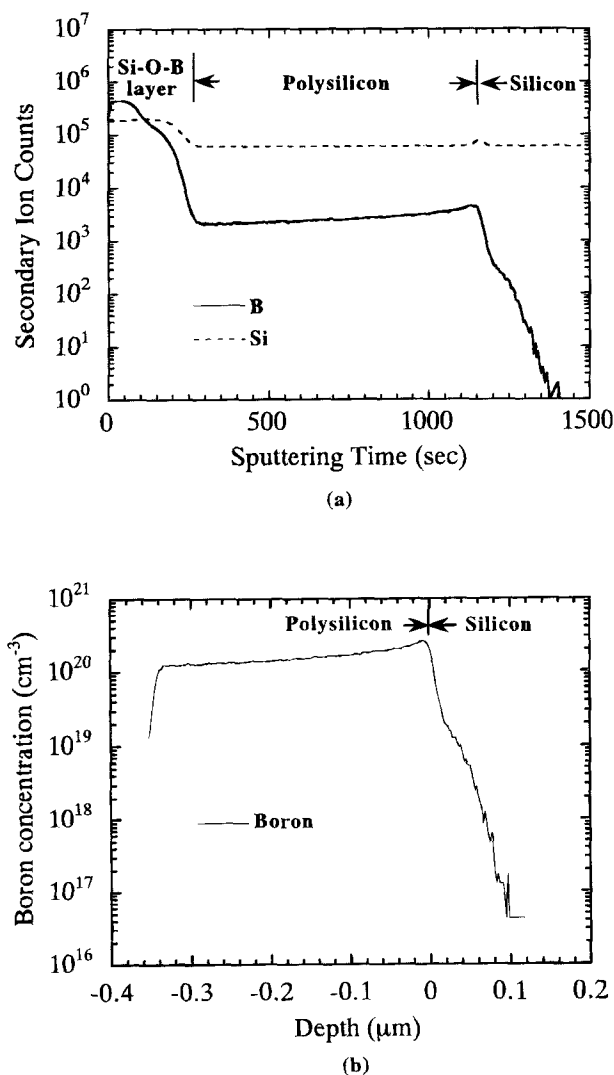


Fig. 5. (a) SIMS boron profile vs. sputtering time for Si-B layer/polysilicon/silicon system after thermal annealing at 900°C for 35 min in an N₂ ambient and 5 min in a wet O₂ ambient. (b) SIMS boron depth profile of (a) after removing the Si-B oxide layer.

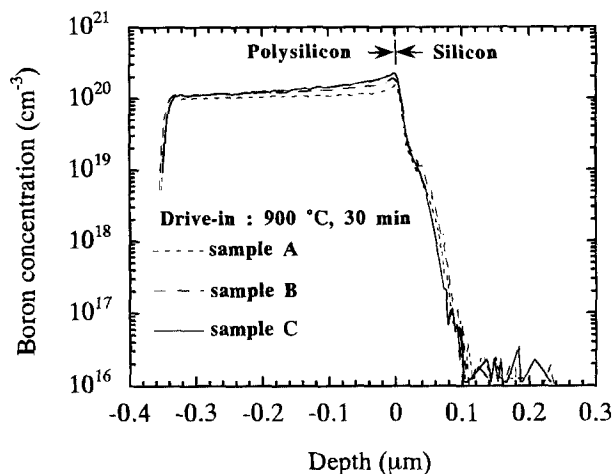


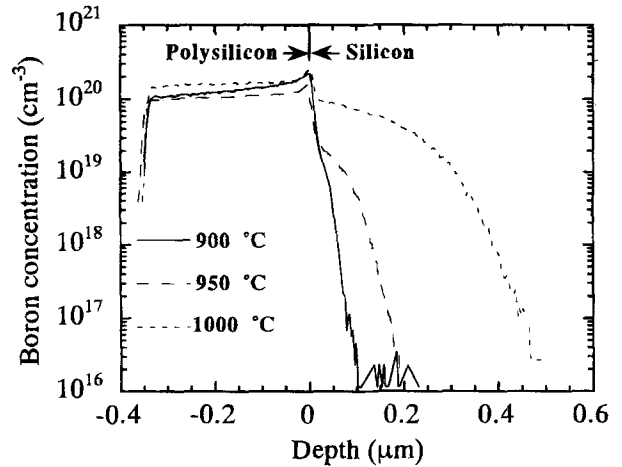
Fig. 6. SIMS boron depth profiles of samples A, B, and C in the polysilicon/silicon after removing the Si-B oxide layer.

polysilicon grain boundary region with a segregation coefficient of 0.7. The polysilicon contacted p⁺-n shallow junction formation with process of A, B, and C has been fabricated. The electrical properties of diodes with process C are better than those of diodes with processes A and B. The results suggest that the drive-in process of C is more suitable for high performance device fabrication.

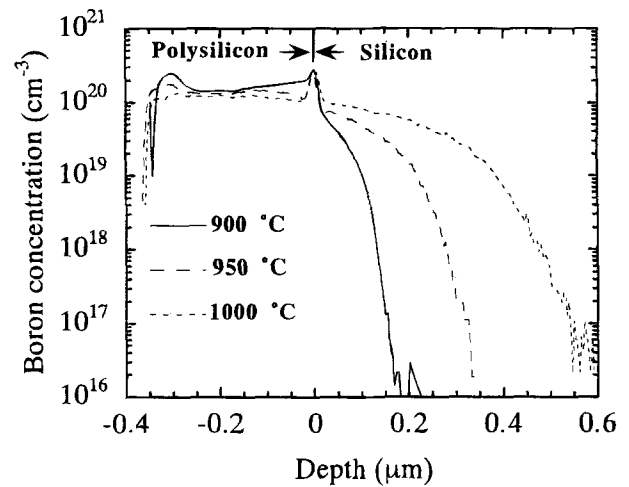
Comparison of grain sizes in Si-B and BF₂ samples.— Figure 7a and b show the plan views of TEM micrograph of polysilicon films for Si-B layer source and BF₂ implanted-polysilicon source, respectively. The samples were annealed at 900°C for 30 min. The average grain size of polysilicon for Si-B layer source is much larger than that of BF₂ implanted-polysilicon source, as observed from a comparison with Fig. 7a and b. A larger polysilicon grain size for Si-B layer source samples is explained by the effects of excess concentration of silicon self-interstitial generation and diffusion into polysilicon during Si-B layer wet oxidation.^{22,23} The silicon self-interstitials are known to have a short diffusion length in polysilicon because they are captured at grain boundaries. The absorption of silicon self-interstitial at polysilicon grain boundaries rendered the grain boundaries mobile and secondary grain growth. Further, it has been reported that the generation of silicon self-interstitial increases with the oxide growth rate.²⁴ In our experiment, the Si-B layer exhibits a much higher oxidation rate than undoped polysilicon. A large amount of silicon self-interstitial can be injected into polysilicon during Si-B layer oxidation and a larger grain size can be obtained for Si-B layer source. In addition, it is well known that the impurity of oxygen atoms can be incorporated into the polysilicon film during deposition. The incorporation of oxygen atoms in the polysilicon films can inhibit secondary grain growth during subsequent high temperature annealing and increase sheet resistance by reducing both Hall mobility and carrier concentration.²⁵ In our experiment, the SIMS oxygen depth profile shows that the counts of oxygen atoms of LPCVD deposition films are much higher than the UHV/CVD deposition films. This is attributed to the background partial pressure of oxygen in the LPCVD system being higher than the UHV/CVD system. After thermal annealing, most oxygen atoms in the polysilicon films diffused into Si-B layer and the counts of oxygen in the Si-B layer is higher than the LPCVD polysilicon films.²⁶ The results indicate that the secondary grain growth can be enhanced for Si-B layer as diffusion source during subsequent high temperature annealing due to the gettering of oxygen by the Si-B layer. Therefore, a larger polysilicon grain size can be obtained by using Si-B layer as diffusion source.

Comparison of boron profiles for Si-B layer source and BF₂-implanted polysilicon source.— In the following inves-

tigations, we have compared boron diffusion in the polysilicon/silicon from Si-B layer source and BF_2^- -implanted polysilicon source. Figure 8a shows the boron depth profiles for Si-B layer source after the thermal drive-in at 900, 950, and 1000°C for 30 min. The Si-B layer oxidation time was properly chosen depending on the drive-in temperature. The oxide layer was removed after thermal drive-in. The surface boron concentration, C_s , value can be obtained by the linear extrapolation of boron profiles in the silicon toward the polysilicon/silicon interface.^{15,16} The surface boron concentration at the silicon side of the interface was increased with drive-in temperature. The phenomenon is more pronounced for drive-in temperatures ranging from 950 to 1000°C. From the SIMS boron profiles, the junction depths were estimated to be 0.05, 0.14, and 0.35 μm for 900, 950, and 1000°C, respectively. Figure 8b show the boron depth profiles in the polysilicon/silicon for BF_2^- -implanted

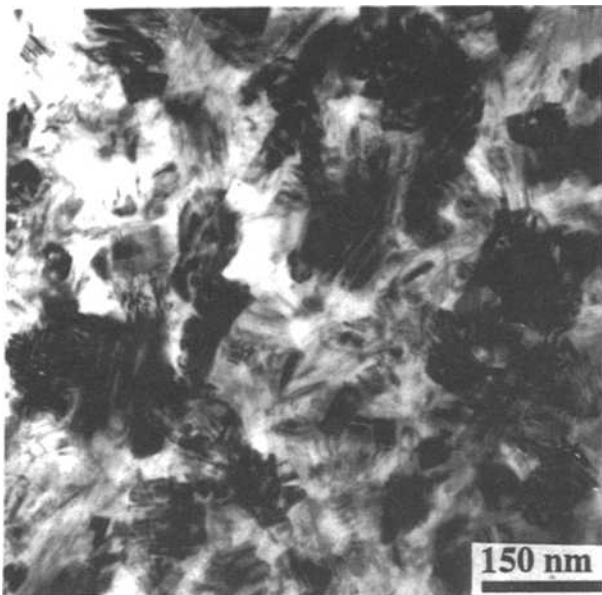


(a)

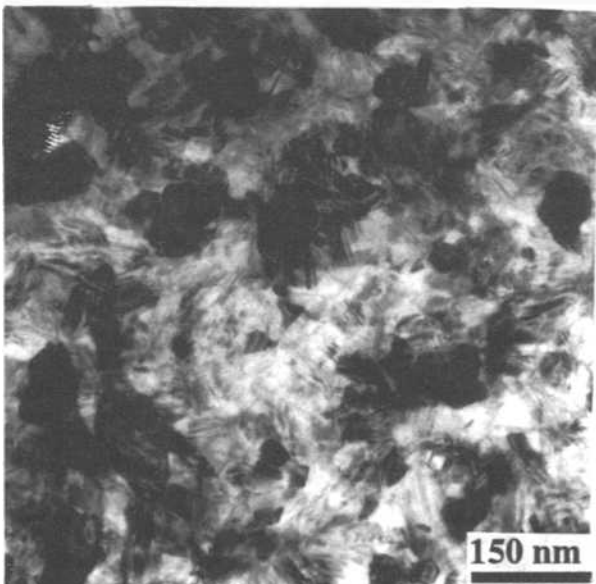


(b)

Fig. 8. SIMS boron depth profiles for (a) Si-B layer source (b) BF_2^- -implanted polysilicon source after thermal drive-in at 900, 950, and 1000°C for 30 min.



(a)



(b)

Fig. 7. The plan views of TEM micrograph of polysilicon films for (a) Si-B layer source and (b) BF_2^- -implanted polysilicon source.

polysilicon source after thermal drive-in at 900, 950, and 1000°C for 30 min. The boron diffusion profiles in the silicon substrates for BF_2^- -implanted polysilicon source are much deeper than those of Si-B layer source, as observed from a comparison with Fig. 8a and b. The junction depths for Si-B layer source samples are much shallower and less sensitive to the drive-in temperature. The C_s values for BF_2^- -implanted polysilicon source are larger than those of Si-B layer source for each drive-in temperature. The results indicate that the C_s values are dependent on the diffusion source. Figure 9a and b shows the boron depth profiles in the polysilicon/silicon for Si-B layer source and BF_2^- -implanted polysilicon source after thermal drive-in at 950°C for several diffusion times. The junction depths for Si-B layer source are much shallower and less sensitive to the annealing time than those of BF_2^- -implanted polysilicon source, as observed from a comparison with Fig. 9a and b. Moreover, the C_s values for two types of diffusion source are independent of diffusion time. That is, the C_s values for two types of diffusion source are dependent on drive-in temperature and independent of drive-in time. For a constant diffusion source, the junction depth is usually approximated by

$$X_j = K(D_s t)^{1/2} \quad [1]$$

where K is a numerical constant, and D_s is the effective boron diffusivity. It has been reported that the effective diffusion constant D_s seems to increase more than linearly with interface concentration C_s for boron diffusion in the polysilicon/silicon.¹⁶ Therefore, according to Eq. 1, the

deeper junction depth for BF_3 -implanted polysilicon source is considered to be due to the larger C_s value. The SIMS fluorine depth profiles showed a fluorine peak at the polysilicon/silicon interface for BF_3 -implanted polysilicon source. As mentioned previously, the pileup of fluorine atoms at the polysilicon/silicon interface has the effect of accelerating the breakup of polysilicon/silicon interfacial oxide and epitaxial regrowth of polysilicon films. For example, the XTEM micrographs showed that the interfacial oxide layer was completely broken up and 30% polysilicon film was epitaxially aligned with silicon for BF_3 -implanted polysilicon as diffusion after thermal annealing at 950°C for 30 min.⁹ In addition, the fluorine bubbles were observed at the polysilicon/silicon interface.⁹ Therefore, the larger C_s value for BF_3 -implanted polysilicon source is considered to be the fluorine effect. In contrast, Fig. 10a, b, and c show the XTEM micrographs of polysilicon/silicon structure for Si-B layer source samples after thermal annealing at 900, 950, and 1000°C for 30 min, respectively. The XTEM micrographs of Fig. 10a and b show that the epitaxial alignment of polysilicon film does not occur for 900 and 950°C annealed samples. However, as shown in Fig. 10c, the interfacial oxide was partially broken up and the polysilicon films were partially epitaxially aligned with silicon for the 1000°C annealed sample. The maximum thickness of the epitaxial alignment of polysilicon film was estimated to be 280 Å. The partial epitaxial alignment of polysilicon film may lead to the rapid increase in surface boron concentration for annealing temperatures ranging from 950 to 1000°C .

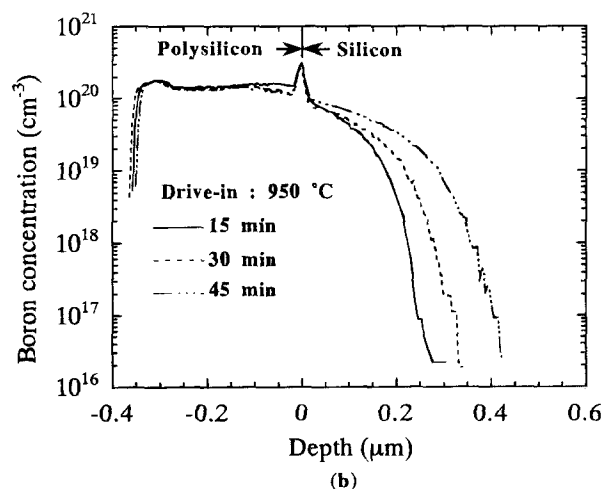
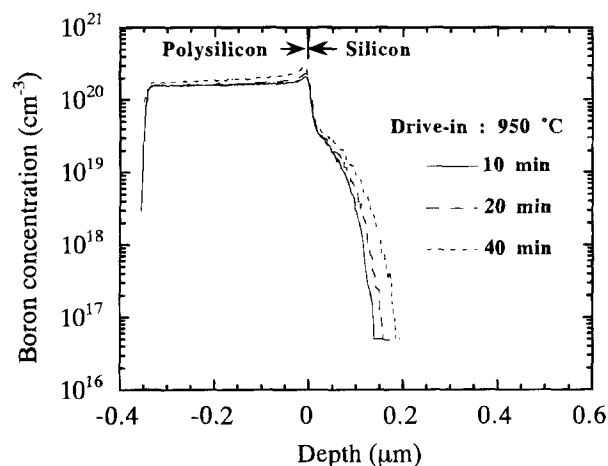
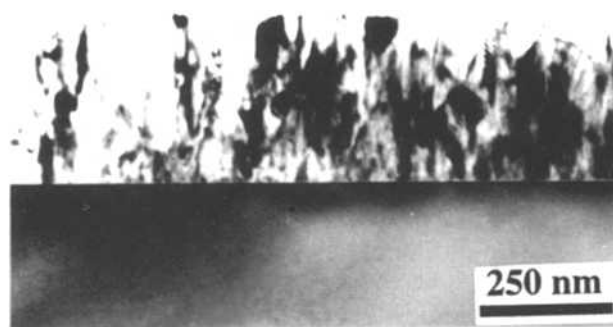
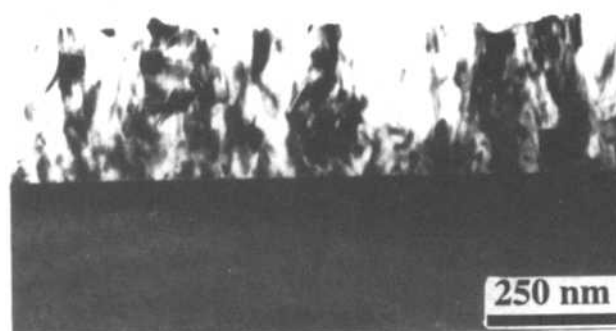


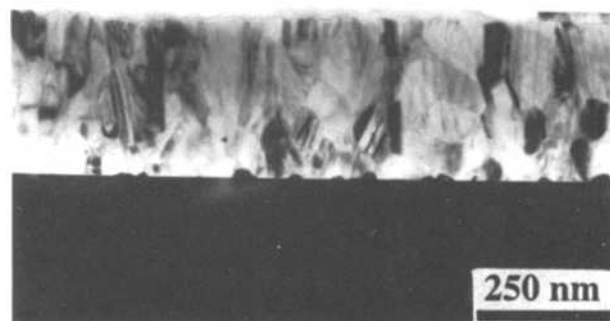
Fig. 9. SIMS boron depth profiles in the polysilicon/silicon for (a) Si-B layer source (b) BF_3 -implanted polysilicon source after thermal drive-in at 950°C for several diffusion times.



(a)



(b)



(c)

Fig. 10. The XTEM micrographs of polysilicon/silicon structure for Si-B layer source samples after thermal annealing at (a) 900°C , (b) 950°C , and (c) 1000°C for 30 min.

Conclusion

The characteristics of boron diffusion in the polysilicon/silicon system with a 350 Å thick Si-B layer as diffusion source have been investigated. The boron diffusion profiles within the polysilicon exhibited a gradual increase of boron concentration toward the polysilicon/silicon interface. The phenomenon possibly is caused by the effect of nonuniform grain size distribution and the segregation of boron atoms in the polysilicon. To obtain high performance devices, a drive-in process for Si-B layer source was suggested. A larger polysilicon grain size for Si-B layer source is attributed to be the effects of the gettering of oxygen impurity by the Si-B layer and secondary grain growth during the wet oxidation of Si-B layer. Moreover, the junction depths for Si-B layer source are much shallower and less sensitive to thermal budget than those of BF_3 -implanted polysilicon source. This is explained by the effect of the smaller surface concentration, C_s , for Si-B layer source.

Acknowledgment

The authors thank W. Y. Hsieh for TEM micrographs. This work was supported by the National Science Council of the Republic of China under Contract No. NSC 83-0404-E009-006.

Manuscript submitted June 28, 1994; revised manuscript received Sept. 30, 1994.

National Chiao Tung University assisted in meeting the publication costs of this article.

REFERENCES

1. A. K. Kapoor and D. J. Roulston, *Polysilicon Emitter Bipolar Transistors*, IEEE Press, New York (1989).
2. P.-F. Lu, J. D. Warnock, J. D. Cressler, K. A. Jenkins, and K.-Y. Toh, *IEEE Trans. Electron Devices*, **ED-38**, 1410 (1991).
3. I. R. C. Post and P. Ashburn, *ibid.*, **ED-38**, 2442 (1991).
4. S. L. Wu, C. L. Lee, T. F. Lei, and H.-C. Chang, *ibid.*, **ED-40**, 1797 (1992).
5. V. Probst, H. J. Bohm, H. Schaber, H. Oppolzer, and I. Weitzel, *This Journal*, **135**, 671 (1988).
6. K. Park, S. Batra, and S. Banerjee, *ibid.*, **138**, 545 (1991).
7. G. D. Williams and P. Ashburn, *J. Appl. Phys.*, **72**, 3169 (1992).
8. S. L. Wu, C. L. Lee, T. F. Lei, and H.-C. Chang, *IEEE Trans. Electron Devices Lett.*, **EDL-13**, 1332 (1992).
9. T. P. Chen, T. F. Lei, C. Y. Chang, W. Y. Hsieh, and L. J. Chen, To be published.
10. H. Schaber, R. V. Criegden, and I. Weitzel, *J. Appl. Phys.*, **58**, 4036 (1985).
11. B. Garben, W. A. Orr-Arienzo, and R. L. Lever, *This Journal*, **133**, 2152 (1986).
12. T. P. Chen, T. F. Lei, H. C. Lin, C. Y. Chang, W. Y. Hsieh, and L. J. Chen, *Appl. Phys. Lett.*, **64**, 1853 (1994).
13. T. P. Chen, T. F. Lei, H. C. Lin, and C. Y. Chang, To be published.
14. D. Graf, M. Drudndner, and R. Schulz, *J. Vac. Sci.*, **A7**, 808 (1989).
15. W. K. Hofker, H. W. Werner, D. P. Oosthoek, and N. J. Koeman, *Appl. Phys.*, **2**, 265 (1973).
16. H. Ryssel, K. Muller, K. Habberger, R. Henkelmann, and F. Jahnelt, *ibid.*, **22**, 35 (1980).
17. W. A. Orr-Arienzo, R. Glang, R. L. Lever, R. K. Lewis, and F. F. Morehead, *J. Appl. Phys.*, **63**, 117 (1988).
18. F. Lau, *IEDM*, 737 (1990).
19. W. A. Rausch, R. F. Lever, and R. H. Kastal, *J. Appl. Phys.*, **54**, 4405 (1983).
20. H. C. Lin, H. Y. Lin, C. Y. Chang, T. F. Lei, P. J. Wang, R. C. Deng, J. Lin, and C. Y. Chao, *Appl. Phys. Lett.*, **63**, 1525 (1993).
21. E. Arai, H. Nakamura, and Y. Terunuma, *This Journal*, **120**, 980 (1973).
22. D. A. Smith and T. Y. Tan, *Mater. Res. Soc. Symp. Proc.*, **5**, 65 (1982).
23. T. Kamins, *Polycrystalline Silicon for Integrated Circuit Applications*, Kluwer Academic, Boston (1988).
24. D. A. Antonialis, *This Journal*, **129**, 1093 (1982).
25. T. I. Kamins and J. E. Turner, *Solid State Technol.*, **80** (1990).
26. T. P. Chen, T. F. Lei, H. C. Lin, C. Y. Chang, J. H. Lin, and L. J. Chen, To be published.